

---

This is an electronic reprint of the original article.  
This reprint may differ from the original in pagination and typographic detail.

Lebedev, A. A.; Davydov, V. Y.; Usachov, D. Y.; Lebedev, S. P.; Smirnov, A. N.; Levitskii, V. S.; Eliseyev, I. A.; Alekseev, P. A.; Dunaevskiy, M. S.; Rybkin, A. G.; Novikov, S. N.; Makarov, Yu N.

## Study of properties and development of sensors based on graphene films grown on SiC (0001) by thermal destruction method

*Published in:*  
Journal of Physics: Conference Series

*DOI:*  
[10.1088/1742-6596/951/1/012007](https://doi.org/10.1088/1742-6596/951/1/012007)

Published: 30/01/2018

*Document Version*  
Publisher's PDF, also known as Version of record

*Published under the following license:*  
CC BY

*Please cite the original version:*  
Lebedev, A. A., Davydov, V. Y., Usachov, D. Y., Lebedev, S. P., Smirnov, A. N., Levitskii, V. S., Eliseyev, I. A., Alekseev, P. A., Dunaevskiy, M. S., Rybkin, A. G., Novikov, S. N., & Makarov, Y. N. (2018). Study of properties and development of sensors based on graphene films grown on SiC (0001) by thermal destruction method. *Journal of Physics: Conference Series*, 951(1), Article 012007. <https://doi.org/10.1088/1742-6596/951/1/012007>

---

This material is protected by copyright and other intellectual property rights, and duplication or sale of all or part of any of the repository collections is not permitted, except that material may be duplicated by you for your research use or educational purposes in electronic or print form. You must obtain permission for any other use. Electronic or print copies may not be offered, whether for sale or otherwise to anyone who is not an authorised user.

PAPER • OPEN ACCESS

## Study of properties and development of sensors based on graphene films grown on SiC (0001) by thermal destruction method

To cite this article: A A Lebedev *et al* 2018 *J. Phys.: Conf. Ser.* **951** 012007

View the [article online](#) for updates and enhancements.

# Study of properties and development of sensors based on graphene films grown on SiC (0001) by thermal destruction method

A A Lebedev<sup>1,2</sup>, V Y Davydov<sup>1</sup>, D Y Usachov<sup>3</sup>, S P Lebedev<sup>1</sup>, A N Smirnov<sup>1,2</sup>, V S Levitskii<sup>1</sup>, I A Eliseyev<sup>1,3</sup>, P A Alekseev<sup>1</sup>, M S Dunaevskiy<sup>1</sup>, A G Rybkin<sup>3</sup>, S N Novikov<sup>4</sup> and Yu N Makarov<sup>5,6</sup>

<sup>1</sup> Ioffe Institute, Russian Academy of Sciences, St. Petersburg, 194021 Russia

<sup>2</sup> ITMO University, St. Petersburg, 197101 Russia

<sup>3</sup> Saint Petersburg State University, St. Petersburg, 199034 Russia

<sup>4</sup> Aalto University, Tietotie 3, 02150, Espoo, Finland

<sup>5</sup> GK «Nitride Crystals», 194156, St. Petersburg, Russia

<sup>6</sup> Nitride Crystals Inc., 181 E Industry Court, Suite B, Deer Park, NY 11729, USA

e-mail: shura.lebe@mail.ioffe.ru

**Abstract.** The structural, chemical, and electronic properties of epitaxial graphene films grown by thermal decomposition of the Si-face of a semi-insulating 6H-SiC substrate in an argon environment are studied by Raman spectroscopy, X-ray photoelectron spectroscopy and angle-resolved photoemission. It was demonstrated the possibility of fabrication of the gas and biosensors that is based on grown graphene films. The gas sensors are sufficiently sensitive to NO<sub>2</sub> at low concentrations. The biosensor operation was checked using an immunochemical system comprising fluorescein dye and monoclonal anti fluorescein antibodies. The sensor detects fluorescein concentration on a level of 1–10 ng/mL and bovine serum albumin–fluorescein conjugate on a level of 1–5 ng/mL. The proposed device has good prospects for use for early diagnostics of various diseases.

## 1. Introduction

Graphene (single layer of graphite) is presently the object of extensive studies due to its unique physical properties and huge potential in the development of new-generation devices that implement the principles of ballistic electronics, spintronics, optoelectronics, nanoplasmonics, and other promising alternatives to conventional semiconductor electronics [1]. For graphene to be economically feasible and attractive for numerous applications, it is necessary to have largesize wafers of high-quality homogeneous graphene. The sublimation of silicon from a semi-insulating single-crystal silicon carbide (SiC) substrate is one of the most promising ways to epitaxially grow graphene [2, 3]. A great advantage of the given technology is that there is no need to transfer the resulting film onto an insulator substrate, as this is done, e.g., in the synthesis of graphene on metals. In addition, this growth technique can grow graphene on the surface of commercial SiC substrates with a diameter of up to 4 in., the industrial manufacture of which has been mastered. Structures of this kind can be used in the standard technological line for the fabrication of semiconductor devices.

The structural characteristics of graphene films strongly depend on which face of SiC crystals they are grown [2, 4]. Films of graphene grown on the C face are commonly constituted by several



mutually misoriented single layers, with their surface topography having the form of separate flakes. By contrast, films grown on the Si face have a more uniform surface structure, which has the form of long terraces with width of  $\sim 1\text{--}2\ \mu\text{m}$ . As a rule, films of this kind are constituted by a single layer, or a small number of these. Thus, the morphological and structural characteristics of graphene films grown on the Si face of SiC are more favorable for the development of devices on their basis.

The goal of our study is the systematic integrated diagnostics of graphene films produced by thermal decomposition of the Si face of a 6H-SiC substrate in order to relate the structural, chemical, and electronic properties of the films to the technological growth parameters.

## 2. Samples and experimental

To obtain graphene films, we used the method of the thermal decomposition of a SiC surface. In contrast to [5, 6], where graphene was grown in a high vacuum, we used the modified growth technique in an inert gas (argon), which enables more precise control over the sublimation of silicon-carbide components. As a consequence, it is possible to control with high precision both the growth process of a graphene film and the uniformity of coating a substrate with graphene.

As substrates served high-resistivity 6H-SiC wafers (manufactured by Svetlana OAO) with  $(0001) \pm 0.25^\circ$  orientation (Si face). Graphene was grown in a graphite crucible inductively heated by a high-frequency generator. To determine the optimal conditions of graphene synthesis, we varied the main technological parameters: the growth temperature was in the range from 1750 to 1900°C; the growth duration was 10 to 30 min; the argon pressure in the growth chamber was 600 to 800 Torr; and the sample heating rate was 100 to 350°C/min.

The structural, chemical, and electronic characteristics of the graphene being grown were monitored by Raman spectroscopy, X-ray photoelectron spectroscopy (XPS), and angle-resolved photoemission spectroscopy (ARPES).

Raman measurements were performed at room temperature in the backscattering configuration using a LabRam HR 800 spectrometer installation equipped with a confocal microscope, which could provide information from a part of the graphene film  $\sim 1\ \mu\text{m}$  in diameter. Together with performing local diagnostics, we analyzed large sample areas ( $10 \times 10$  to  $30 \times 30\ \mu\text{m}$ ), with the subsequent plotting of Raman maps of the spectral line parameters. This procedure made it possible to carry out one of the main tasks of the present study, which consisted in assessing the uniformity of the structural characteristics over the sample area. We used in these measurements an excitation light wavelength of 532 nm and a laser power of 2.0 mW on a sample in a spot  $\sim 1\ \mu\text{m}$  in diameter at a spectrometer resolution of  $2.5\ \text{cm}^{-1}$ .

ARPES, and XPS data with  $\text{AlK}_\alpha$  radiation were obtained at the Resource Centre “Physical Methods of Surface Investigation” of the Research Park of Saint Petersburg State University (SPbU). The XPS spectra at various photon energies were measured with synchrotron radiation at the Russian-German beam line of the BESSY II synchrotron radiation facility.

Below results that are typical of samples grown in the final stage of optimization of the technological parameters are presented.

## 3. Graphen films structural characterization

### 3.1. Raman data

Figure 1a shows an array of Raman spectra measured in the spectral range  $1300\text{--}2800\ \text{cm}^{-1}$  on a sample area of  $12.5 \times 12.5\ \mu\text{m}^2$ . The spectra show features appearing upon light scattering from the graphene film: *G* and *2D* lines and a weak *D* line [7]. The Raman diagnostics of graphene layers is based on an analysis of the frequency position, width, and intensity ratio of the *G*, *2D*, and *D* lines in the spectra. Analysis of the *G* line intensity map, which was obtained by processing this array, revealed a rather uniform distribution of the line intensity over the sample area. This is indicative of good thickness uniformity of the graphene film in the region being analyzed. It was found that the *2D* line is symmetric in the majority of spectra and is well fitted by a single Lorentzian, which is a fingerprint of a single-layer graphene [7]. The shape of the *2D* line which can be approximated by an envelope of four Lorentzians is observed in no more than 10% of the total number of spectra in the

array. It follows from these data that the sample being analyzed is mostly formed by single-layer graphene with a small number of double-layer inclusions. The ratio between the integral intensities of  $D$  and  $G$  lines ( $I_D/I_G$ ) can be used to evaluate the structural perfection of a graphene film. It was found that the  $I_D/I_G$  ratio distribution has a maximum at around 0.08, which corresponds to a defect concentration of  $N_d < 10^{10} \text{ cm}^{-2}$  [7]. The compression strain in the graphene layer estimated from the correlation between the positions of the  $G$  and  $2D$  lines is  $\varepsilon_{\parallel} = (0.35 \pm 0.03)\%$ .

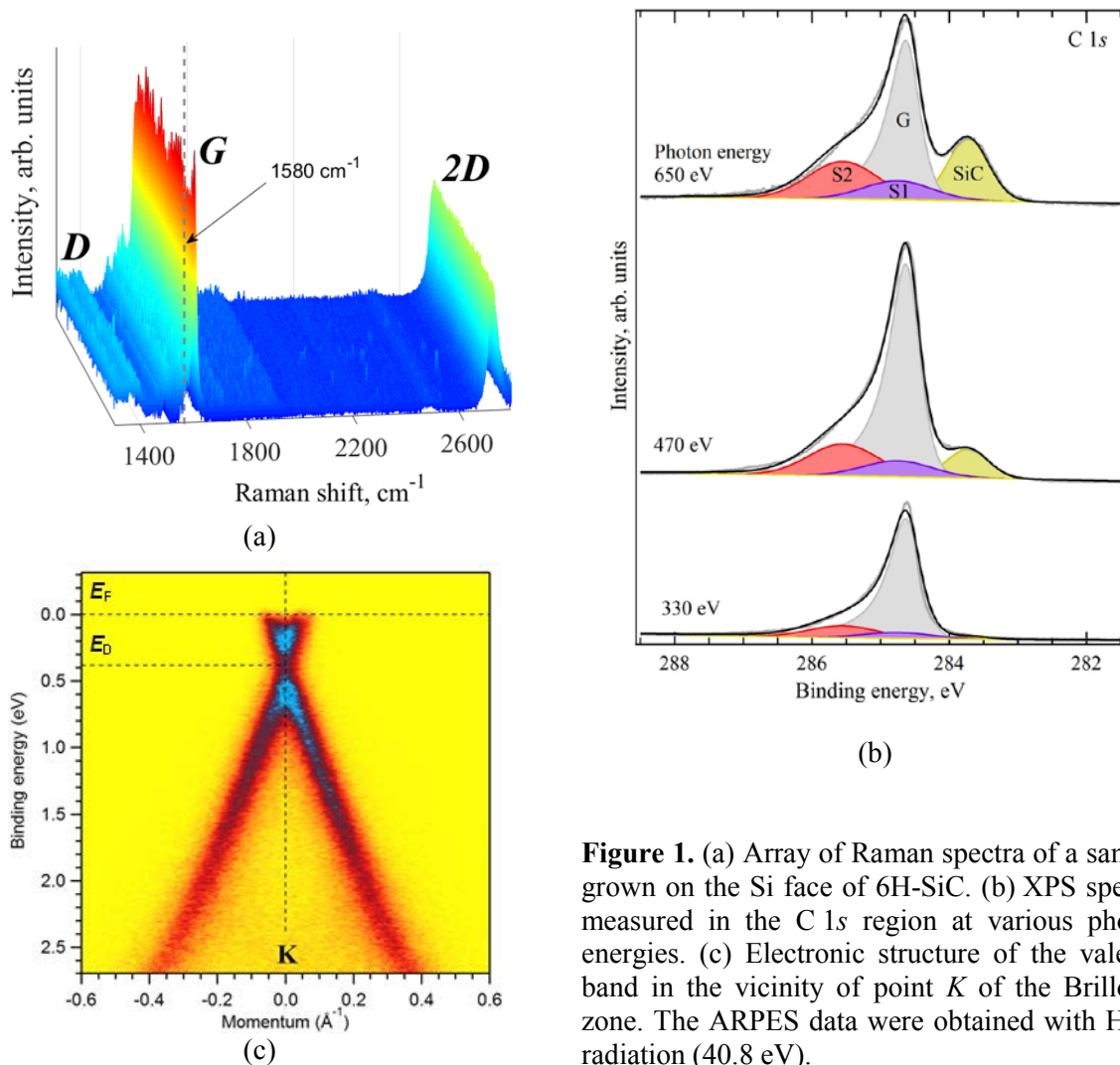


**Figure 1.** (a) Array of Raman spectra of a sample grown on the Si face of 6H-SiC. (b) XPS spectra measured in the C 1s region at various photon energies. (c) Electronic structure of the valence band in the vicinity of point  $K$  of the Brillouin zone. The ARPES data were obtained with He II radiation (40.8 eV).

### 3.2. XPS and ARPES data and Results of Synchrotron Measurements

To determine the chemical composition of the near-surface region, a survey XPS spectrum was measured upon removing molecules adsorbed in air via heating in ultrahigh vacuum at a temperature of  $500^\circ\text{C}$ . Only a small amount of oxygen was found in the spectrum in addition to lines related to carbon and silicon and peaks associated with the characteristic loss of energy by electrons. The content of oxygen in the upper atomic layers of SiC is approximately 1 at %. A detailed analysis of the shape of the XPS data in the region of the C 1s line makes it possible to estimate the average graphene thickness. To reliably determine the thickness of graphene, we analyzed XPS spectra obtained at four photon energies providing different depths of analysis within the range 5–23  $\text{\AA}$  (Figure 1b). The layer thicknesses were determined by choosing those thicknesses of the graphene and buffer layer that

provided the best coincidence between the calculated and measured intensities of separate components of C 1s spectra.

It is known that the electronic structure of the valence band varies with the number of graphene layers. Single-layer graphene is characterized by a Dirac cone of electronic states at point *K* of the Brillouin zone, whereas the formation of a second layer leads to energy splitting of the cone and to doubling of the number of states. The ARPES data for the electronic structure of the valence band of the graphene/SiC(0001) system are shown in Figure 1c. An unsplit Dirac cone is seen at point *K*. This indicates that a single-layer graphene coating is predominant on the surface. This conclusion agrees with the Raman, AFM, and XPS data, according to which a sample grows as predominantly single-layer graphene with a small amount (~10%) of inclusions of double-layer islands with submicrometer dimensions. It is also seen from the ARPES data that the Dirac point lies below the Fermi level and has a binding energy of  $E \approx 0.4$  eV. This unambiguously points to *n*-type doping with an electron concentration in the conduction band of  $n = E^2/\pi(\hbar v_F)^2 \approx 10^{13} \text{ cm}^{-2}$  [8].

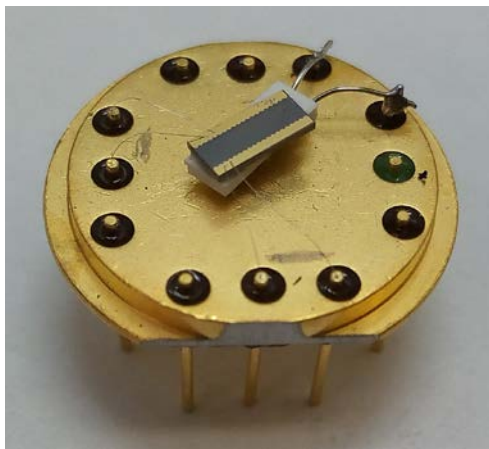


**Figure 2.** Graphene sensor chip on the holder.

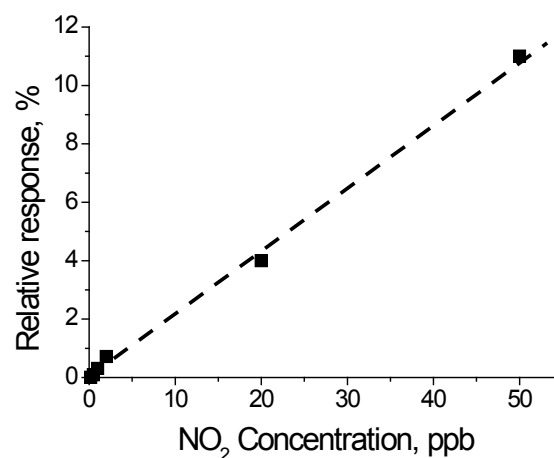


**Figure 3.** Plot of the response of the graphene-based gas sensor vs. NO<sub>2</sub> concentration in gas mixture at a temperature of 20°C.

#### 4. Sensors developing and characterization

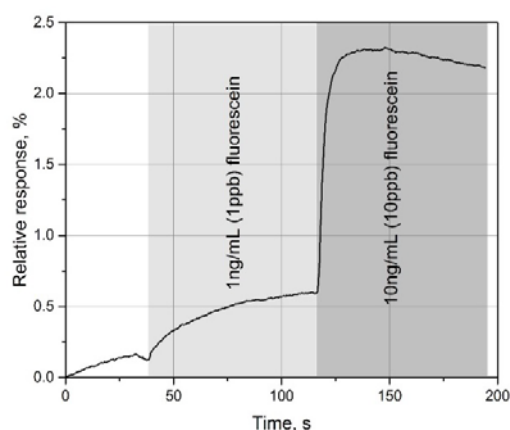
We fabricated the sensor structure on the graphene film using laser photolithography and an AZ5214 photoresist [9,10] (Figure 2). Excess graphene is removed from the substrate surface with the aid of etching in the oxygen–argon plasma. Ti/Au (5/50 nm) ohmic contacts are fabricated using lift-off photolithography after deposition of metal on the surface of photoresist using electron-beam evaporation. The chip of the sensor is fixed on a holder with two Pt100 resistors that are used for temperature measurement and heating, respectively. In the measurements of the sensor sensitivity, we use the existing system for mixing and supply of gas mixtures [9,10]. Such a system allows a variation in the dilution coefficient from 1 : 1 to 1 : 10<sup>5</sup>, so that the output concentration of the detected gas ranges from 0.1 ppb to 10 ppm. Purified air serves as a carrier gas. Sensor sensitivity *r* is measured in percents and determined as a relative variation in the resistance of the sample in the presence of the gas mixture containing the detected gas:

$$r = (R - R_0)/R_0,$$

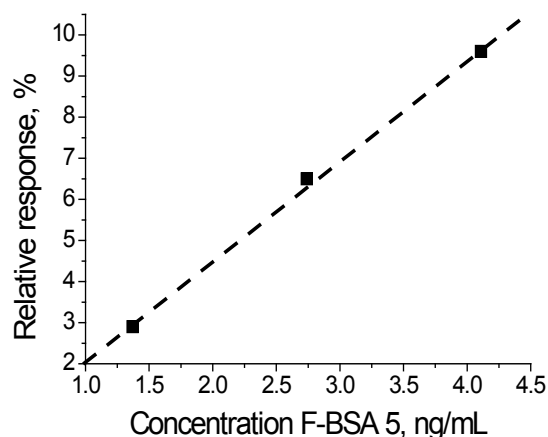
here, *R* is the resistance of the sensor in the presence of the gas and *R*<sub>0</sub> is the original resistance in the absence of the detected gas in the air flow.

Figure 3 shows relative variations in the resistance of the graphene sensor in the presence of NO<sub>2</sub> in the gas mixture at a temperature of 20°C. The desorption rate of NO<sub>2</sub> is extremely low at room temperature. Therefore, annealing at a temperature of 110°C is used to refresh the sensor [9].

It should be noted that a significant disadvantage of graphene-based gas sensors is the lack of selectivity. Indeed, a change in the conductivity does not indicate which particular molecule is adsorbed on the graphene surface. Moreover, some molecules contribute to conductivity with opposite signs, so that the total change in resistance can be nearly zero. The problem of selectivity in graphene-based sensors can be solved by using the antigen–antibody reaction. The components of such a pair can only interact with each other and not with any other protein. As is known, certain stages of many diseases involve the appearance of antigen–markers that are specific of one disorder or a group of several disorders. These antigens may bind to specific antibodies preliminarily immobilized on the surface of a graphene sensor. Then, the antigen–antibody reaction will lead, by analogy with a gas sensor, to a change in resistivity of the graphene film.



**Figure 4.** Variation of graphene-based sensor resistance during contact with solutions containing free fluorescein (at indicated concentrations).



**Figure 5.** Variation of the graphene-based sensor resistance during contact with solutions containing BSA–fluorescein conjugate (F-BSA-5)

The technology of graphene-based biosensors was developed with respect to an immunochemical system comprising fluorescein dye and monoclonal anti-fluorescein antibodies (MAbs), in which the dye can be present both in the form of free molecules and as those chemically conjugated to protein carriers. The molecular mass of fluorescein (0.322 kDa) is comparable to that of some biologically significant marker molecules, such as hormones, nucleotides, and short peptides.

The measurements were carried out in borate buffer solution. The results of testing graphene-based sensors with anti-FITC MAbs grafted on the surface showed that the sensor resistance exhibited clearly detected changes upon contact with solutions containing low-molecular-mass ligands at concentrations of 1 and 10 ng/mL (Figure 4). Tests with high-molecular-mass ligands were performed using specially prepared bovine serum albumin (BSA) conjugated to fluorescein (F-BSA-5). The molecular mass of F-BSA-5 conjugate (69 kDa) is comparable to those of proteins used as markers of human diseases. In the F-BSA-5 conjugate, each fluorescein group accounts for about 5% of the total molecular mass. According to spectrophotometric data, the conjugate used in this work contained three fluorescein groups per F-BSA-5 molecule. When in contact with the solution of high-molecular-mass ligands (F-BSA-5), changes in the electric resistance of the graphene-based sensor were detected at conjugate concentrations within 1.37–3.11 ng/mL (Figure 5).

## 5. Conclusions

The results of an integrated study related the structural, chemical, and electronic characteristics of graphene films grown by the method of thermal decomposition of the SiC surface to the technological growth modes. This made it possible to optimize the technological parameters and develop a reproducible growth technology of single-layer graphene films with a small fraction of fine inclusions of double-layer graphene on the Si face of 6H-SiC substrates. It was found that the best structural

characteristics are observed for graphene films grown with the following technological parameters: growth temperature of 1850°C; growth duration of 10 min; argon pressure in the growth chamber of 750 Torr; sample heating rate of 100–150°C/min. On the whole, the samples can be characterized as high-quality graphene, which enables the development of devices on the basis of these samples.

Also, we have demonstrated the possibility of fabrication of a gas sensor that is based on grapheme grown with the aid of sublimation in vacuum. The sensors are sufficiently sensitive to NO<sub>2</sub> at low concentrations. The results can be used in commercial production of graphene sensors.

At present, the diagnostics of human diseases is based to a significant degree on determining the concentrations and/or presence of certain marker molecules in the blood, which are specific to one or a group of disorders. The detection of diagnostically significant amounts of marker macromolecules is now performed using laborious, time-consuming procedures of enzyme immunoassay. The use of graphene-based biosensors may provide an accelerated and technically advanced approach to diagnostics of human diseases.

### Acknowledgments

This work was financially supported by the Ministry of Education and Science of the Russian Federation (agreement No 14.575.21.0148, unique identifier of applied scientific research RFMEFI57517X0148).

### References

- [1] Ferrari A C *et al.* 2015 *Nanoscale* **7** 4598
- [2] Emtsev K V *et al.* 2009 *Nat. Mater.* **8** 203
- [3] Yazdi G R, Iakimov T and Yakimova R 2016 *Crystals* **6** 53
- [4] Tedesco J L, VanMil B, Myers-Ward R, McCrate J M, Kitt S A, Campbell P M, Jernigan G G, Culbertson J C, Eddy Jr. C R and Gaskill D K 2009 *Appl. Phys. Lett.* **95** 122102
- [5] Agrinskaya N V, Berezovets V A, Kozub V I, Kotousova I S, Lebedev A A, Lebedev S P, and Sitnikova A A 2013 *Semiconductors* **47** 301
- [6] Lebedev A A, Lebedev S P, Novikov S N, Davydov V Yu, Smirnov A N, Litvin D P, Makarov Yu N and Levitskii V S 2016 *Tech. Phys.* **61** 453
- [7] Ferrari A C and Basko D M 2013 *Nature Nanotech.* **8** 235
- [8] Davydov V Yu, Usachov D Yu, Lebedev S P, Smirnov A N, Levitskii V S, Elisseyev I A, Alekseev P A, Dunaevskiy M S, Vilkov O Yu, Rybkin A G and Lebedev A A 2017 *Semiconductors* **51** 1072
- [9] Novikov S, Lebedeva N and Satrapinski A 2015 *J. Sensors* **2015** 108581
- [10] Novikov S, Lebedeva N, Satrapinski A, Walden J, Davydov V and Lebedev A 2016 *Sens. Actuators B: Chem.* **236** 1054